

Washington University School of Medicine

Digital Commons@Becker

Open Access Publications

2017

The emergence of network inefficiencies in infants with autism spectrum disorder

John R. Pruett Jr.

Washington University School of Medicine in St. Louis

Kelly N. Botteron

Washington University School of Medicine in St. Louis

Robert C. McKinstry

Washington University School of Medicine in St. Louis

et al

Follow this and additional works at: https://digitalcommons.wustl.edu/open_access_pubs

Please let us know how this document benefits you.

Recommended Citation

Pruett, John R. Jr.; Botteron, Kelly N.; McKinstry, Robert C.; and et al, "The emergence of network inefficiencies in infants with autism spectrum disorder." *Biological Psychiatry*. 82, 3. 176-185. (2017). https://digitalcommons.wustl.edu/open_access_pubs/6759

This Open Access Publication is brought to you for free and open access by Digital Commons@Becker. It has been accepted for inclusion in Open Access Publications by an authorized administrator of Digital Commons@Becker. For more information, please contact vanam@wustl.edu.

The Emergence of Network Inefficiencies in Infants With Autism Spectrum Disorder

John D. Lewis, Alan C. Evans, John R. Pruett Jr., Kelly N. Botteron, Robert C. McKinstry, Lonnie Zwaigenbaum, Annette M. Estes, D. Louis Collins, Penelope Kostopoulos, Guido Gerig, Stephen R. Dager, Sarah Paterson, Robert T. Schultz, Martin A. Styner, Heather C. Hazlett, and Joseph Piven, for the Infant Brain Imaging Study Network

ABSTRACT

BACKGROUND: Autism spectrum disorder (ASD) is a developmental disorder defined by behavioral features that emerge during the first years of life. Research indicates that abnormalities in brain connectivity are associated with these behavioral features. However, the inclusion of individuals past the age of onset of the defining behaviors complicates interpretation of the observed abnormalities: they may be cascade effects of earlier neuropathology and behavioral abnormalities. Our recent study of network efficiency in a cohort of 24-month-olds at high and low familial risk for ASD reduced this confound; we reported reduced network efficiencies in toddlers classified with ASD. The current study maps the emergence of these inefficiencies in the first year of life.

METHODS: This study uses data from 260 infants at 6 and 12 months of age, including 116 infants with longitudinal data. As in our earlier study, we use diffusion data to obtain measures of the length and strength of connections between brain regions to compute network efficiency. We assess group differences in efficiency within linear mixed-effects models determined by the Akaike information criterion.

RESULTS: Inefficiencies in high-risk infants later classified with ASD were detected from 6 months onward in regions involved in low-level sensory processing. In addition, within the high-risk infants, these inefficiencies predicted 24-month symptom severity.

CONCLUSIONS: These results suggest that infants with ASD, even before 6 months of age, have deficits in connectivity related to low-level processing, which contribute to a developmental cascade affecting brain organization and eventually higher-level cognitive processes and social behavior.

Keywords: Autism, Connectivity, Development, Efficiency, Infant siblings, Network analysis

<http://dx.doi.org/10.1016/j.biopsych.2017.03.006>

Autism spectrum disorder (ASD) is a developmental disorder defined by impairments in social communication and social interaction and a restricted repertoire of activities and interests (1). A great deal of research has focused on relating these behavioral symptoms to brain-based measures to understand how neurological abnormalities give rise to the symptoms of ASD. The majority of this research, however, has been based on adults, adolescents, and older children, but the behavioral manifestations of ASD first appear during the first or second year of life (2–5). Differences in the brains of individuals with ASD who are far past this age may be the result of a complex cascade of effects compounding some early neuropathology with the progressive impact of this neuropathology and its associated behaviors on brain development. These results therefore tell us little about the emergence of the neuropathology that is associated with the earliest behavioral signs of ASD. To elucidate this, we study brain development during infancy.

In a recent study (6), we sought to determine what, if any, differences in structural networks were present around the age

at which the characteristic symptoms of autism consolidate (2–5). Motivated by recent research relating abnormalities in brain connectivity in ASD to a number of the behavioral features (7–25), we assessed white matter connectivity differences in 24-month-old siblings of older children diagnosed with ASD, who are known to be at high familial risk for ASD, as well as 24-month-olds at low familial risk for ASD (i.e., with no first-degree relative with ASD or intellectual disability). We assessed regional abnormalities in network efficiency in ASD (i.e., the capacity to exchange information across a network) and the relation between these regional differences and symptom severity. Our results showed significantly decreased efficiency in regions of the temporal, parietal, and occipital lobes, and in Broca's area in high-risk infants classified as having ASD. This was among the earliest evidence of atypical connectivity in ASD, reported at an age when diagnosis first becomes feasible and stable (26–28).

The current study aims to map the emergence of these network inefficiencies earlier in development, before symptom

SEE COMMENTARY ON PAGE 152

consolidation (28,29). We use magnetic resonance imaging data together with clinical diagnosis and measures of symptom severity (28). As in our earlier study, we obtain tractography-based measures of the length and strength of connections between anatomical brain regions and assess the efficiency of information transfer for each brain region to all other brain regions and within local subnetworks (30–33). These measures simultaneously capture differences in the strengths of the connections between brain regions and differences in the spatial organization of the brain. We assess differences in these measures of efficiency for every region of the brain in infants with ASD versus non-ASD infants, as well as the relation between efficiency and symptom severity. To ascertain the developmental progression, we measure these effects over time.

METHODS AND MATERIALS

Here we present an abbreviated version of the methods; a detailed version can be found in the [Supplement](#).

Participants

Participants were drawn from the Infant Brain Imaging Study, an ongoing multisite longitudinal study funded by the National Institutes of Health Autism Centers of Excellence program. The Infant Brain Imaging Study documents brain and behavioral development in infants at high familial risk for ASD by virtue of having an older sibling with ASD, as well as in infants deemed to be at low familial risk for ASD by virtue of having no first-degree relative with ASD or intellectual disability and an older sibling.

Neuroimaging and behavioral data were collected from high and low familial risk infants at 6, 12, and 24 months of age. The data acquired included T1- and T2-weighted images and diffusion data. Usable data were acquired from 260 infants:

116 infants with longitudinal data, 33 infants for whom all imaging data were available at 6 months of age and structural but not diffusion data were available at 12 months, and 111 infants for whom all imaging data were available at 12 months of age but not at 6 months. These data were stratified by risk status and according to whether or not they received a diagnosis of ASD at 24 months of age. [Table 1](#) provides the sample characteristics for high-risk infants diagnosed with ASD (HR^{POS}), high-risk infants diagnosed as not having ASD (HR^{NEG}), and low-risk infants diagnosed as not having ASD (LR^{NEG}). Note that much of the data are from LR^{NEG} and HR^{NEG} infants, limiting the power of the analysis of group differences. The analysis of the relation between efficiency and symptom severity does not suffer this limitation because it uses both the HR^{POS} and HR^{NEG} infants.

Behavioral Assessment

A clinical best-estimate diagnosis was made by two clinicians based on all available information to determine whether a participant met the DSM-IV-TR criteria for autistic disorder, pervasive developmental disorder not otherwise specified, or neither. ASD symptom severity was derived from the Autism Diagnostic Observation Schedule (34) according to Gotham *et al.* (35). The means and standard deviations of the symptom severity scores for each group are reported in [Table 1](#).

Imaging and Image Processing

Magnetic resonance imaging scans were performed while infants were naturally sleeping. Data were collected at each site on Siemens 3T TIM Trio scanners (Siemens Medical Solutions, Malvern, PA) with 12-channel head coils. T1-, T2-, and diffusion-weighted images were collected.

T1- and T2-weighted images were subjected to a visual quality control during postprocessing. The diffusion-weighted

Table 1. Sample Characteristics of the Study Groups

	HR^{POS}		HR^{NEG}		LR^{NEG}	
	<i>n</i>	Age, Months (Mean ± SD)	<i>n</i>	Age, Months (Mean ± SD)	<i>n</i>	Age, Months (Mean ± SD)
V06						
Male	15	6.7 ± 0.8	47	6.6 ± 0.7	40	6.8 ± 0.7
Female	2	6.7 ± 0.4	33	6.7 ± 0.8	12	6.5 ± 0.5
V12						
Male	27	12.8 ± 0.8	77	12.6 ± 0.5	37	12.7 ± 0.6
Female	2	12.9 ± 0.6	62	12.7 ± 0.7	22	12.9 ± 0.9
V06 + V12						
Male	13	—	39	—	27	—
Female	2	—	27	—	8	—
	ADOS Severity (Mean ± SD)		ADOS Severity (Mean ± SD)		ADOS Severity (Mean ± SD)	
V06, V12, V06 + V12						
Male	—	5.3 ± 2.3	—	1.4 ± 0.8	—	1.4 ± 1.0
Female	—	7.0 ± 1.2	—	1.5 ± 1.1	—	1.2 ± 0.6

V06 rows provide the sample sizes and ages (in months) at the 6-month visit for individuals for whom there are only 6-month efficiency measures and individuals for whom there are longitudinal measures. Likewise, the V12 rows provide the sample sizes and ages at the 12-month visit for individuals for whom there are only 12-month efficiency measures and individuals for whom there are longitudinal measures. V06 + V12 rows provide the sample size for the longitudinal portion of the sample.

ADOS, Autism Diagnostic Observation Schedule; HR^{NEG} , high-risk infants diagnosed as not having autism spectrum disorder; HR^{POS} , high-risk infants diagnosed with autism spectrum disorder; LR^{NEG} , low-risk infants diagnosed as not having autism spectrum disorder.

images were cleaned of motion and other artifacts using DTI-Prep (36), which corrects artifacts where possible, and excludes directions from the data when correction is not possible. Further visual quality control potentially eliminated additional artifacts. If this process excluded >20% of the directions for any size subset of the largest b-values, the dataset was deemed unacceptable. Only datasets with acceptable T1-, T2-, and diffusion-weighted images were included in the analysis.

The T1 and T2 volumes were corrected for geometric distortion (37) and then processed with CIVET, a fully automated structural image analysis pipeline developed at the Montreal Neurological Institute. The contrast in the 6-month data is insufficient for CIVET to extract accurate surfaces, so 6-month data were included in the analysis only if the 12-month T1 and T2 volumes were acceptable.

The CIVET results were used to construct the seed, stop, and target masks for use with FSL's *probtrackx* (38). Seed masks were the entire white matter. Stop masks were the voxels on the boundary of the white matter. Target masks consisted of the cortical labels of the DKT40 surface parcellation (39), as well as subcortical labels defined on a template derived from pediatric data (40).

After artifact rejection and motion correction with DTIPrep (36), the diffusion-weighted images were unwarped to the distortion-corrected T2 volume. Two copies of these data were then preprocessed for probabilistic tractography with FSL's *bedpostx* (38): one in native space, and one scaled to the 12-month template. Connection lengths were estimated using the native space data; connection strengths were estimated using the scaled data. The unwarped diffusion volumes were affine registered to the T1 volumes in stereotaxic space. Probabilistic tractography using FSL's *probtrackx* was then seeded from each voxel of the seed masks, with and without distance bias correction (38,41), both in native and in 12-month standard space. These results were then compiled for each region of the cortical parcellation, generating undirected matrices of the total number of connections between each pair of regions from the results in standard space and the mean physical length of those connections from the results in native space. The total number of connections between each pair of regions of the parcellation divided by the average surface area of the two regions in stereotaxic space is referred to as connection "strength."

Analysis

We performed a longitudinal analysis of network efficiency using the methods developed in our previously reported analysis of the 24-month data (6). Based on Rubinov and Sporns (42), we define the weighted distance between nodes i and j as

$$d_{ij}^w = \sum_{u,v \in S_{ij}} \frac{d_{uv}}{w_{uv}}$$

where S_{ij} is the shortest path, in terms of tractography-based measures of physical distances, between nodes i and j ; d_{uv} is the length of the edge between u and v along that path, and w_{uv} is the connection strength between nodes u and v . The

shortest paths, in terms of weighted distances, have "transmission times" that decrease with the strengths of the connections involved and increase with the tractography-based measures of the physical distances involved. Our weighted formulations of nodal global efficiency and nodal local efficiency, also based on Rubinov and Sporns (42), are

$$E_{nodal\ global}^{weighted}(G, i) = \frac{1}{(N-1)} \sum_{j \in G, j \neq i} (d_{ij}^w)^{-1}$$

where N is the number of nodes in the network graph G ; and d_{ij}^w is the shortest path, in terms of weighted distance, between nodes i and j ; and

$$E_{nodal\ local}^{weighted}(G, i) = \frac{1}{N_{G_i}(N_{G_i}-1)} \sum_{j \neq k \in G_i} \left((d_{jk}^w)^{-1} w_{ij} w_{ik} \right)^{1/3}$$

where N_{G_i} is the number of nodes in the subgraph G_i consisting of all of the neighbors of i ; d_{jk}^w is the shortest path, in terms of weighted distance, between nodes j and k ; and w_{ij} and w_{ik} are the connection strengths between nodes i and j and i and k , respectively. According to Latora and Marchiori (30), these measures are normalized by considering the fully connected network.

Differences in nodal local efficiency and nodal global efficiency between infants with ASD and non-ASD infants were assessed via mixed-effects linear models. The group of non-ASD infants was based on clinical best-estimate diagnosis, ignoring familial risk (i.e., combines the LR^{NEG} and HR^{NEG} infants). At each node, the best-fit model was determined by the Akaike information criterion with the data centered at 9 months of age (43,44). In addition to subject-specific random effects, the models could control for any of the following: age, age², sex, site, age × sex, age² × sex, age × group, and age² × group. All possible models were evaluated, and group differences were assessed within the model with the lowest Akaike information criterion value. Group differences were assessed across time to evaluate how the models differed by group over development. Group differences were assessed with the data centered at 6, 9, and 12 months of age.

Finally, to determine the extent to which network structure might explain individual behavioral differences—both across individuals with ASD and across the broader autism phenotype (45–48)—we assessed the relation between the measures of network efficiency and the Autism Diagnostic Observation Schedule-calibrated severity scores (35) across all high-risk infants. This was also assessed at each node within the model with the lowest Akaike information criterion value; in this case, with models that could control for site and any of severity, age, age², and sex, and interactions of these terms with each other and with severity.

In all analyses, we use a false discovery rate (FDR) correction for multiple comparisons (49).

RESULTS

Relative to the non-ASD infants, HR^{POS} infants showed reductions in nodal local efficiency from 6 months of age onward (Figure 1; Supplemental Table S1). The HR^{POS} infants showed FDR-corrected significant reductions in nodal local

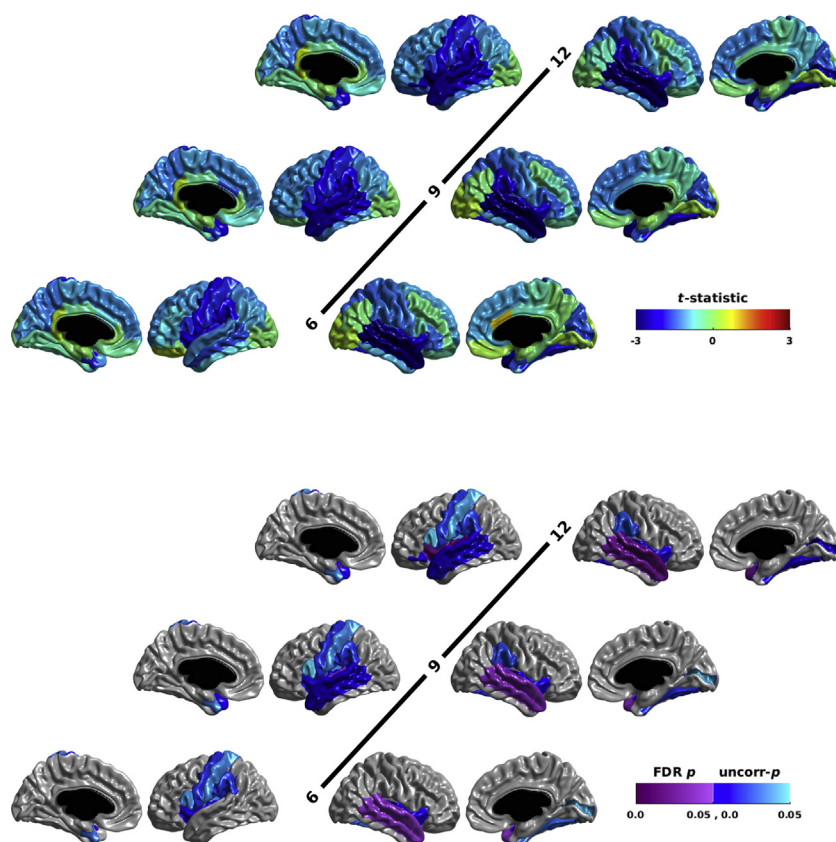


Figure 1. The group differences in nodal local efficiency for high-risk infants diagnosed with autism spectrum disorder vs. high-risk infants diagnosed as not having autism spectrum disorder and low-risk infants diagnosed as not having autism spectrum disorder assessed at 6, 9, and 12 months of age. The t statistic is shown in the top half of the figure; the p statistic is shown in the bottom half. Reduced efficiency in high-risk infants diagnosed with autism spectrum disorder yields a negative t statistic (blue); increased efficiency yields a positive t statistic (red). The p statistic maps show both the p values that survive a false discovery rate (FDR) correction for multiple comparisons (purple), as well as those that are significant uncorrected, but do not survive multiple comparison correction (blue). Each row shows the results for the left hemisphere on the left and the right hemisphere on the right. The medial views for the left hemisphere are furthest to the left; the medial views for the right hemisphere are furthest to the right. Age is indicated in the center of each row. Note that false discovery rate-significant reductions in nodal local efficiency in high-risk infants diagnosed with autism spectrum disorder are seen at 6 months of age in the right primary auditory cortex and superior and middle temporal gyri; reductions in the left primary auditory cortex become significant by 9 months of age, followed by reductions in the left insula by 12 months of age.

efficiency over the right primary auditory cortex and the superior and middle temporal gyri from 6 months of age onwards. With the data centered at 9 months of age, the HR^{POS} infants showed FDR-corrected significant reductions in the left primary auditory cortex as well, and also in the left insula with the data centered at 12 months of age. This development of group differences was reflected in the models for these regions; both included an $\text{age}^2 \times \text{group}$ interaction term. Note that all group differences at all time points were reductions in nodal local efficiency in HR^{POS} infants.

Relative to the non-ASD infants, the HR^{POS} infants also showed reductions in nodal global efficiency (Figure 2; Supplemental Table S2). HR^{POS} infants showed an FDR-corrected significant reduction in nodal global efficiency only in Broca's area at 12 months of age. The emergence of this group difference was reflected in the $\text{age}^2 \times \text{group}$ interaction term in this region. As with nodal local efficiency, all group differences at all time points were reductions in nodal global efficiency in HR^{POS} infants.

Across the high-risk infants, the measures of network efficiency and the symptom severity scores were inversely related (i.e., symptom severity increased with decreasing efficiency). There were FDR significant inverse relations of symptom severity to nodal local efficiency from 6 months of age onward, and no significant positive correlations at any time point (Figure 3; Supplemental Table S3). At 6 months of age, the inverse relations between severity and nodal local efficiency reached FDR-corrected significance in the left primary auditory

cortex and the right superior temporal gyrus. By 9 months of age, the inverse relation in the left primary visual cortex reached FDR significance, as well as the left insula and supramarginal and superior temporal gyri, and the middle temporal gyri bilaterally. By 12 months of age, the inverse relation in bilateral medial visual cortex reached FDR significance, as well as the left somatosensory cortex and angular gyrus, the right insula, and superior parietal lobule. Though the left primary auditory cortex showed a significant relation between nodal local efficiency and severity from 6 months onward, the relationship strengthened with age, as reflected by the t statistic; this developmental change in the relationship was reflected in an $\text{age}^2 \times \text{severity}$ interaction term in the model for this region. The strengthening relationships between nodal local efficiency and severity seen in the bilateral insula, the right cuneus and superior parietal lobule, and the left somatosensory cortex and angular gyrus were also reflected in $\text{age}^2 \times \text{severity}$ interaction terms in the models for those regions.

The emerging relations between symptom severity and nodal global efficiency were also exclusively inverse relations (Figure 4; Supplemental Table S4). The inverse relations first reached FDR significance at 9 months of age in the right somatosensory cortex and angular gyrus and the supramarginal gyrus bilaterally. The emergence of these relationships in each of these regions was reflected in an $\text{age} \times \text{sex} \times \text{severity}^2$ interaction term in the models, and for the right angular gyrus, also an $\text{age} \times \text{sex} \times \text{severity}$ interaction term.

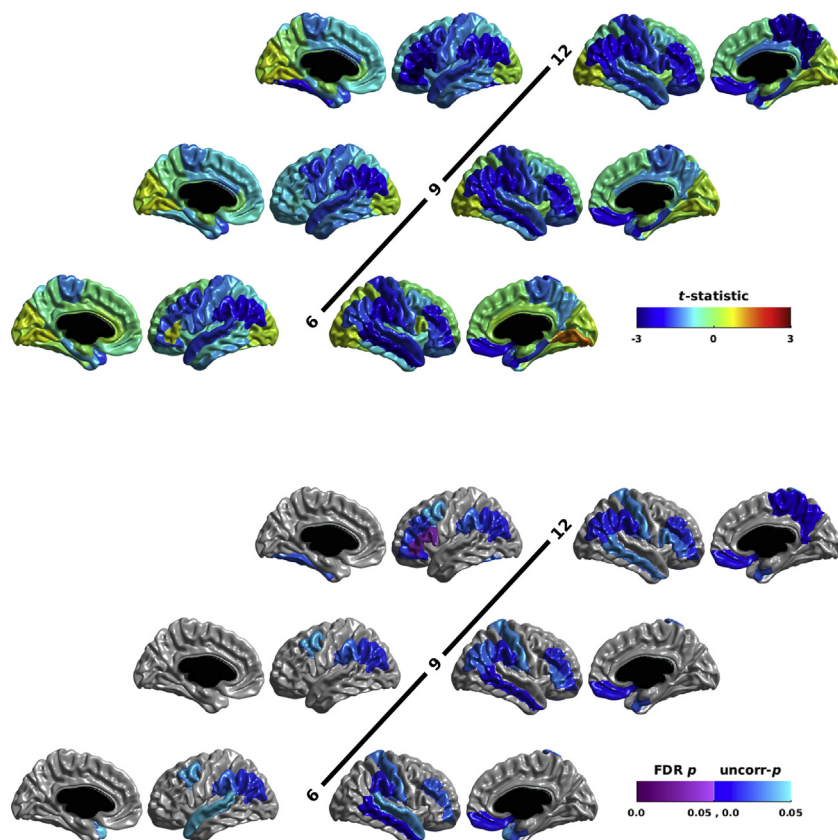


Figure 2. The group differences in nodal global efficiency for high-risk infants diagnosed with autism spectrum disorder vs. high-risk infants diagnosed as not having autism spectrum disorder and low-risk infants diagnosed as not having autism spectrum disorder assessed at 6, 9, and 12 months of age. The t statistic is shown in the top half of the figure; the p statistic is shown in the bottom half. Reduced efficiency in high-risk infants diagnosed with autism spectrum disorder yields a negative t statistic (blue); increased efficiency yields a positive t statistic (red). The p statistic maps show both the p values that survive a false discovery rate (FDR) correction for multiple comparisons (purple), as well as those that are significant uncorrected, but do not survive multiple comparison correction (blue). Each row shows the results for the left hemisphere on the left and the right hemisphere on the right. The medial views for the left hemisphere are furthest to the left; the medial views for the right hemisphere are furthest to the right. Age is indicated in the center of each row. Note that false discovery rate-significant reductions in nodal global efficiency in high-risk infants diagnosed with autism spectrum disorder are seen in Broca's area at 12 months of age.

By 12 months of age, there were FDR significant inverse relations in bilateral somatosensory cortex, the left motor cortex, and supplementary motor cortex, as well as Broca's area and its right hemisphere homologue, the bilateral supra-marginal and angular gyri, and the right precuneus, medial orbitofrontal cortex, and middle frontal gyrus. The emergence of the additional relations seen at 12 months of age in Broca's area and its right hemisphere homologue, as well as the left motor cortex and right precuneus and medial orbitofrontal cortex, are again reflected in an age \times sex \times severity² interaction term in the models for these regions.

Notably, both for the analyses of the group differences in efficiency and for the relation of efficiency to symptom severity, the best-fit model for the majority of nodes included age as a covariate, and in all cases, age was significantly positively related to efficiency.

DISCUSSION

Our previous analysis of network efficiency in 24-month-olds showed reductions in efficiency in ASD and an inverse relation between efficiency and symptom severity within the high-risk group. Our goal in the current analysis was to map the emergence of these network inefficiencies during the first year of life in infants who go on to develop ASD, in order to identify more precisely where and when these inefficiencies first appear. Our results show inefficiencies already present at 6 months of age in regions associated with auditory processing, and by 12 months

of age in additional regions known to be involved in low-level processing and integration, as well as Broca's area, a region involved in more abstract aspects of language processing. In addition, across high-risk infants, lower network efficiency at 6 months of age in regions encompassing primary and secondary auditory areas was associated with greater 24-month symptom severity; and over the next 6 months, visual, somatosensory, and motor areas, as well as areas involved in sensory integration and higher-level processing (e.g., Broca's and Wernicke's areas), also became associated with 24-month symptom severity. Children and adults with ASD, and in the broader autism phenotype, commonly have abnormalities in motor behaviors, responses to tactile, auditory, and visual stimuli, and in their processing of language and nonlinguistic social stimuli (e.g., faces) as well as in higher-level cognitive processes [e.g., executive function (45–48,50–60)]. Both this pattern of emergence of reductions in efficiency in infants who go on to develop ASD and the pattern of emergence of inverse relations between efficiency and 24-month symptom severity are consistent with the conjecture that some of the most developmentally proximal deficits in ASD, and in the broader autism phenotype, are in low-level sensory processing (61) rather than higher-level cognitive processes (14,62,63), and that abnormalities in higher-level processes (e.g., language) stem from these low-level inefficiencies. It should be noted, however, that inclusion of the cerebellum and subcortical regions in the analysis may alter the results, particularly given their importance in sensory and motor processing (64–66).

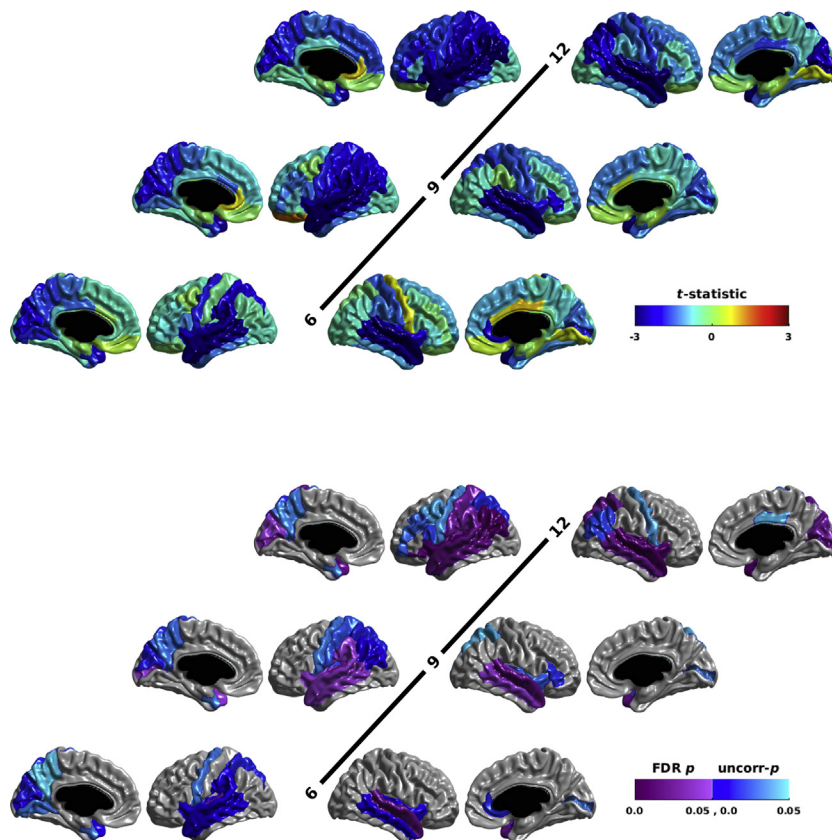


Figure 3. The relation of autism severity scores to nodal local efficiency in the high-risk infants, assessed within linear mixed effects models at 6, 9, and 12 months of age. The t statistic is shown in the top half of the figure; the p statistic is shown in the bottom half. A positive correlation between efficiency and severity yields a positive t statistic (red); an inverse relation between efficiency and severity yields a negative t statistic (blue). The p statistic maps show both the p values that survive a false discovery rate (FDR) correction for multiple comparisons (purple), as well as those that are significant uncorrected but do not survive multiple comparison correction (blue). Each row shows the results for the left hemisphere on the left and the right hemisphere on the right. The medial views for the left hemisphere are furthest to the left; the medial views for the right hemisphere are furthest to the right. Age is indicated in the center of each row. Note that there are false discovery rate–significant inverse relations between autism severity and nodal local efficiency at 6 months of age in primary auditory cortex, and that by 12 months of age there are also inverse relations in visual and somatosensory regions, as well as the insula.

We have suggested that findings reported for cohorts that included older children, adolescents, or adults would, at least in part, reflect cascade effects of earlier abnormalities in neural circuitry and behavioral abnormalities, rather than representing the primary neural underpinnings of the disorder. Our previous analysis of network efficiency in 24-month-olds reduced the possibility that the observed abnormalities were contaminated by cascade effects from earlier neuropathology or behavioral abnormalities, but did not eliminate that possibility (6). The current analysis further reduces that possible confound. The fact that significant reductions in efficiency are seen in infants with ASD by 6 months of age indicates that neural abnormalities are present before the onset of the defining behavioral features of autism. To date, infant studies have not been able to identify behavioral markers of the defining features of ASD before 12 months of age (67–70). In addition, within the Infant Brain Imaging Study sample, the HR infants with ASD show no abnormalities in the social communication or repetitive behaviors domains at 6 months of age (28); however, those with high 24-month severity scores do show abnormalities in sensorimotor behaviors (28). This appears to be reflected in the pattern of reductions in efficiency at 6 months of age. Though there are reductions in efficiency already at 6 months of age in HR infants with ASD, those reductions are only associated with primary auditory cortex and the superior and middle temporal gyri; likewise, efficiency at 6 months of age is associated with 24-month symptom severity only for the primary auditory cortex and the superior temporal gyrus. These results suggest

that reductions in efficiency in frontal regions (71) typically associated with higher-level cognitive processes (e.g., executive function) may be cascade effects from these earlier deficits in regions supporting lower-level processing of sensory inputs (61). Such cascade effects might underlie findings of parametric relationships between social communicative symptoms of autism and brain responses in nonsocial perceptual decision tasks (72). Inefficiencies in regions associated with higher-level cognitive functions might, of course, arise independently, potentially because of the same neuropathology affecting regions involved in low-level sensory processing (61); but neural abnormalities that yield basic level deficits early in development are likely to have cascade effects over developmental time through interactions within the brain, altered interactions with the environment, and altered gene expression (73).

It is important to note, however, that regional differences in efficiency indicate differences not in the nodes themselves but in the networks associated with those nodes. Therefore, reduced efficiency in early sensory processing regions does not mean that those regions, in isolation, are deficient; but rather that the structure of the network is less optimal for those regions. In addition, nodal local and nodal global efficiency are not simply indices of connectivity, implying abnormalities in short- and long-range connectivity, respectively. The reductions in both nodal local and nodal global efficiency in HR^{POS} infants more likely reflect a more random configuration than seen in the non-ASD infants, having less of the modular structure seen in the typical mature brain. Reductions in nodal

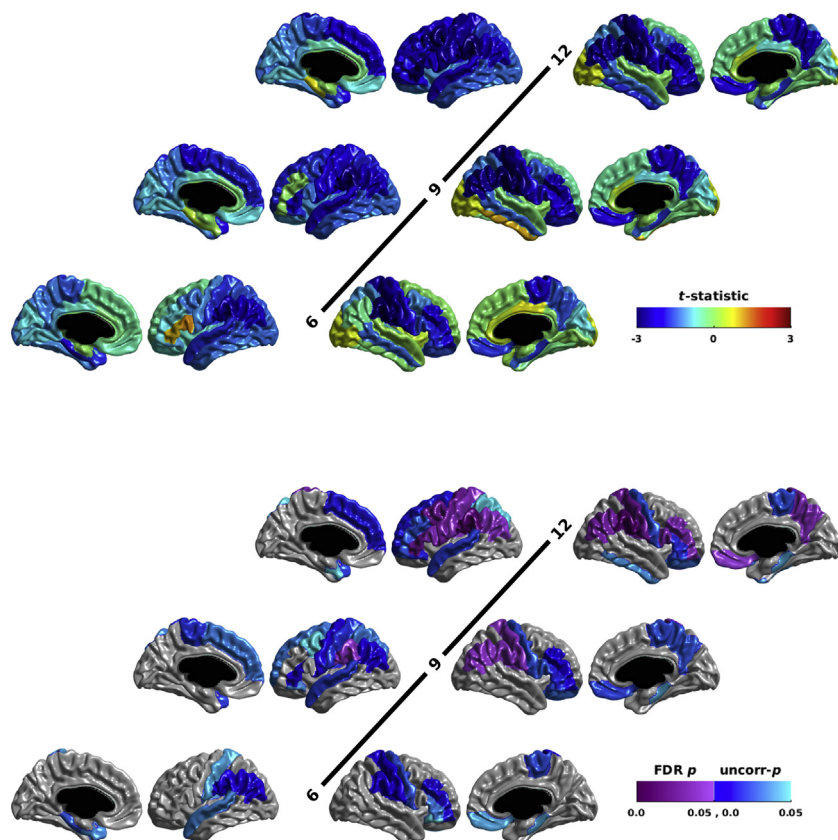


Figure 4. The relation of autism severity scores to nodal global efficiency in the high-risk infants, assessed within linear mixed-effects models at 6, 9, and 12 months of age. The t statistic is shown in the top half of the figure; the p statistic is shown in the bottom half. A positive correlation between efficiency and severity yields a positive t statistic (red); an inverse relation between efficiency and severity yields a negative t statistic (blue). The p statistic maps show both the p values that survive a false discovery rate (FDR) correction for multiple comparisons (purple), as well as those that are significant uncorrected but do not survive multiple comparison correction (blue). Each row shows the results for the left hemisphere on the left and the right hemisphere on the right. The medial views for the left hemisphere are furthest to the left; the medial views for the right hemisphere are furthest to the right. Age is indicated in the center of each row. Note that there are false discovery rate-significant inverse relations between autism severity and nodal global efficiency by 9 months of age in areas involved in somatosensory processing and language processing, and that by 12 months of age there are inverse relations in a more extensive set of language areas, including Broca's area and its right hemisphere homologue, as well as areas involved in motor processing and more abstract aspects of cognition.

local efficiency suggest that corticocortical organization is deficient with respect to the spatial clustering required for rapid processing, whereas reductions in nodal global efficiency suggest that corticocortical organization is deficient with respect to the long-range connectivity that provides for integration of information between different brain regions. The results here indicate that the first deficits in corticocortical organization in infants with ASD are in terms of forming spatially local clusters of regions with strong interconnectivity—specifically clusters including regions involved in auditory processing. We speculate that these deficits in spatial clustering may then lead to reductions in integration with more spatially distant regions (e.g., between temporal or occipital lobe areas involved in low-level processing and frontal lobe areas involved in higher-level processing).

This is not to suggest, however, that there is a single etiology of these initial local deficits. The multitude of genetic mutations associated with autism (74), as well as the behavioral heterogeneity of the disorder, argue otherwise. Nor is it to suggest that the underlying processes are themselves necessarily spatially local; in fact, that reduced nodal local efficiency at 12 months is associated with increased symptom severity at 24 months in regions associated with auditory, visual, and somatosensory processing suggests a general deficit. Multiple mechanisms might alter development timing to yield such an outcome. Children with ASD show reduced developmental synaptic pruning (75,76). Such a decrease in synaptic pruning will hamper the axonal remodeling that refines the massively

exuberant connectivity produced prenatally, resulting in inefficient overconnectivity. Alterations in neurotrophic factors might also yield such an outcome (77). Abnormalities in attention or social reward might also impact neural processing, and in turn, structure (78). The fact that these associations appear first in regions involved in low-level processing may reflect only that development proceeds from primary to secondary to tertiary areas (79,80), or that there is less variability in the way these regions are connected with other regions. Once such deficits in low-level processing exist, however, they will propel an altered developmental cascade, with consequences to downstream neural development. Therefore, without early longitudinal data, it will be difficult to determine whether later seen abnormalities are consequences of such a developmental cascade or instead arise independently.

Perhaps even more important than where in the brain these deficits first arise is when they arise. These results indicate that the neuropathology of ASD must originate before 6 months of age. By 6 months of age, HR infants who go on to develop ASD already show deficiencies in corticocortical organization. This is important for several reasons. First, it suggests that neural biomarkers of ASD could be present before 6 months of age, which might allow for identification presymptomatically. Abnormalities within a developing system give rise to further abnormalities; therefore, intervention later in development is operating on a vastly altered neural landscape, and likely therefore meets with limited success (81–84). Intervention should likely begin

as soon as the first signs of abnormality appear and should be theoretically directed to stem the cascade of abnormalities. Preliminary evidence from animal research suggests that intensive auditory behavioral training may be able to limit or eliminate the abnormalities seen here in auditory cortex (85). Second, such early biomarkers, with little contamination from cascade effects, would provide a way to characterize heterogeneity in the neuropathology associated with ASD, and an improved possibility of linking neuropathology to genetic alterations. Third, the presence of abnormalities at 6 months of age narrows the set of possible environmental triggers, improving our chances of identifying such triggers.

However, it bears repeating that the group differences reported here are based on 31 HR^{POS} infants, of which only two are female, and 15 provide longitudinal data. The results for the analysis of the relation between efficiency and symptom severity provide supporting evidence, and are based on a larger number of infants (i.e., 184 infants, of which 70 are female, and 81 provide longitudinal data). Nonetheless, larger amounts of longitudinal data from even younger infants will be required to determine more precisely, and with greater certainty, when and where the reductions in efficiency first appear in infants who go on to develop ASD.

ACKNOWLEDGMENTS AND DISCLOSURES

This work was supported by National Institutes of Health Grant Nos. R01HD055741 (to JP) and R01MH093510 (to JRP); by Grant BC_Azrieli_MIRI_3388 from the Azrieli Neurodevelopmental Research Program in partnership with the Brain Canada Multi-Investigator Research Initiative (to ACE); and by funding from Autism Speaks (to JP), the Simons Foundation (to JP), and the Canada Foundation for Innovation, the Government of Québec, the National Science and Engineering Research Council, the Fonds Québécois de Recherche sur la Nature et les Technologies, and La Fondation Marcelle et Jean Coutu (to ACE).

The Infant Brain Imaging Study Network is comprised of the following individuals: J. Piven, H.C. Hazlett, C. Chappell, S.R. Dager, A.M. Estes, D. Shaw, K.N. Botteron, R.C. McKinstry, J. Constantino, J.R. Pruett, R.T. Schultz, S. Paterson, L. Zwaigenbaum, J.T. Ellison, A.C. Evans, D.L. Collins, G.B. Pike, V. Fonov, P. Kostopoulos, S. Das, G. Gerig, M.A. Styner, and H. Gu.

We thank the Infant Brain Imaging Study children and families for their ongoing participation in this longitudinal study.

The authors report no biomedical financial interests or potential conflicts of interest.

ARTICLE INFORMATION

From the Montreal Neurological Institute (JDL, ACE, DLC, PK), McGill University, Montreal, Quebec, Canada; Departments of Psychiatry (JRP, KNB) and Radiology (JRP, KNB, RCM), Washington University School of Medicine, Saint Louis, Missouri; Department of Pediatrics (LZ), University of Alberta, Edmonton, Alberta, Canada; Departments of Speech and Hearing Sciences (AME) and Radiology (SRD), University of Washington, Seattle, Washington; Tandon School of Engineering (GG), New York University, Brooklyn, New York; Center for Autism Research (SP, RTS), University of Pennsylvania, Philadelphia, Pennsylvania; and the Department of Computer Science (MAS) and the Carolina Institute for Developmental Disabilities (MAS, HCH, JP), University of North Carolina, Chapel Hill, North Carolina.

Address correspondence to John D. Lewis, Ph.D., McGill University, Montreal Neurological Institute, 3801 University, WB208, Montreal, QC, H3A 2B4, Canada; E-mail: jlewis@bic.mni.mcgill.ca.

Received Jul 22, 2016; revised Feb 27, 2017; accepted Mar 9, 2017.

Supplementary material cited in this article is available online at <http://dx.doi.org/10.1016/j.biopsych.2017.03.006>.

REFERENCES

1. American Psychiatric Association (2013): Diagnostic and Statistical Manual of Mental Disorders, 5th ed. Arlington, VA: American Psychiatric Publishing.
2. Osterling J, Dawson G (1994): Early recognition of children with autism: A study of first birthday home videotapes. *J Autism Dev Disord* 24:247–257.
3. Maestro S, Muratori F, Cavallaro MC, Pei F, Stern D, Golse B, *et al.* (2002): Attentional skills during the first 6 months of age in autism spectrum disorder. *J Am Acad Child Adolesc Psychiatry* 41:1239–1245.
4. Zwaigenbaum L, Bryson S, Rogers T, Roberts W, Brian J, Szatmari P (2005): Behavioral manifestations of autism in the first year of life. *Int J Dev Neurosci* 23:143–152.
5. Brian J, Bryson S, Garon N, Roberts W, Smith I, Szatmari P, *et al.* (2008): Clinical assessment of autism in high-risk 18-month-olds. *Autism* 12:433.
6. Lewis JD, Evans A, Pruett J, Botteron K, Zwaigenbaum L, Estes A, *et al.* (2014): Network inefficiencies in autism spectrum disorder at 24 months. *Transl Psychiatry* 4:e388.
7. Egaas B, Courchesne E, Saitoh O (1995): Reduced size of corpus callosum in autism. *Arch Neurol* 52:794.
8. Just MA, Cherkassky VL, Keller TA, Minshew NJ (2004): Cortical activation and synchronization during sentence comprehension in high-functioning autism: Evidence of underconnectivity. *Brain* 127:1811–1821.
9. Keller TA, Kana RK, Just MA (2007): A developmental study of the structural integrity of white matter in autism. *Neuroreport* 18:23–27.
10. Koshino H, Carpenter PA, Minshew NJ, Cherkassky VL, Keller TA, Just MA (2005): Functional connectivity in an fMRI working memory task in high-functioning autism. *Neuroimage* 24:810–821.
11. Liu Y, Cherkassky VL, Minshew NJ, Just MA (2011): Autonomy of lower-level perception from global processing in autism: Evidence from brain activation and functional connectivity. *Neuropsychologia* 49:2105–2111.
12. Villalobos ME, Mizuno A, Dahl BC, Kemmotsu N, Müller RA (2005): Reduced functional connectivity between V1 and inferior frontal cortex associated with visuomotor performance in autism. *Neuroimage* 25:916.
13. Turner KC, Frost L, Linsenbardt D, McIlroy JR, Müller RA (2006): Atypically diffuse functional connectivity between caudate nuclei and cerebral cortex in autism. *Behav Brain Funct* 2:34.
14. Just MA, Cherkassky VL, Keller TA, Kana RK, Minshew NJ (2007): Functional and anatomical cortical underconnectivity in autism: Evidence from an fMRI study of an executive function task and corpus callosum morphometry. *Cereb Cortex* 17:951–961.
15. Frazier T, Hardan A (2009): A meta-analysis of the corpus callosum in autism. *Biol Psychiatry* 66:935–941.
16. Uddin LQ, Menon V (2009): The anterior insula in autism: Under-connected and under-examined. *Neurosci Biobehav Rev* 33:1198–1203.
17. Murias M, Webb SJ, Greenson J, Dawson G (2007): Resting state cortical connectivity reflected in EEG coherence in individuals with autism. *Biol Psychiatry* 62:270–273.
18. Li H, Xue Z, Ellmore TM, Frye RE, Wong STC (2012): Network-based analysis reveals stronger local diffusion-based connectivity and different correlations with oral language skills in brains of children with high functioning autism spectrum disorders. *Hum Brain Mapp* 35:396–413.
19. Vissers ME, Cohen MX, Geurts HM (2011): Brain connectivity and high functioning autism: A promising path of research that needs refined models, methodological convergence, and stronger behavioral links. *Neurosci Biobehav Rev* 36:604–625.
20. Wilson TW, Rojas DC, Reite ML, Teale PD, Rogers SJ (2007): Children and adolescents with autism exhibit reduced MEG steady-state gamma responses. *Biol Psychiatry* 62:192–197.
21. Barttfeld P, Wicker B, Cukier S, Navarta S, Lew S, Sigman M (2011): A big-world network in ASD: Dynamical connectivity analysis reflects a

- deficit in long-range connections and an excess of short-range connections. *Neuropsychologia* 49:254–263.
22. Belmonte MK, Allen G, Beckel-Mitchener A, Boulanger LM, Carper RA, Webb SJ (2004): Autism and abnormal development of brain connectivity. *J Neurosci* 24:9228–9231.
 23. Noonan SK, Haist F, Müller RA (2009): Aberrant functional connectivity in autism: Evidence from low-frequency BOLD signal fluctuations. *Brain Res* 1262:48–63.
 24. Welchew DE, Ashwin E, Berkouk K, Salvador R, Suckling J, Baron-Cohen S, *et al.* (2005): Functional disconnectivity of the medial temporal lobe in Asperger's syndrome. *Biol Psychiatry* 57:991–998.
 25. Shih P, Shen M, Öttl B, Keehn B, Gaffrey MS, Müller RA (2010): Atypical network connectivity for imitation in autism spectrum disorder. *Neuropsychologia* 48:2931–2939.
 26. Ozonoff S, Young GS, Landa RJ, Brian J, Bryson S, Charman T, *et al.* (2015): Diagnostic stability in young children at risk for autism spectrum disorder: A baby siblings research consortium study. *J Child Psychol Psychiatry* 56:988–998.
 27. Zwaigenbaum L, Bryson SE, Brian J, Smith IM, Roberts W, Szatmari P, *et al.* (2016): Stability of diagnostic assessment for autism spectrum disorder between 18 and 36 months in a high-risk cohort. *Autism Res* 9:790–800.
 28. Estes A, Zwaigenbaum L, Gu H, John TS, Paterson S, Elison JT, *et al.* (2015): Behavioral, cognitive, and adaptive development in infants with autism spectrum disorder in the first 2 years of life. *J Neurodev Disord* 7:24.
 29. Yirmiya N, Charman T (2010): The prodrome of autism: Early behavioral and biological signs, regression, peri- and post-natal development and genetics. *J Child Psychol Psychiatry* 51:432–458.
 30. Latora V, Marchiori M (2001): Efficient behavior of small-world networks. *Phys Rev Lett* 87:198701.
 31. Latora V, Marchiori M (2003): Economic small-world behavior in weighted networks. *Eur Phys J B* 32:249–263.
 32. Achard S, Bullmore E (2007): Efficiency and cost of economical brain functional networks. *PLoS Comput Biol* 3:e17.
 33. Bullmore E, Sporns O (2012): The economy of brain network organization. *Nat Rev Neurosci* 13:336–349.
 34. Lord C, Risi S, Lambrecht L, Cook EH, Leventhal BL, DiLavore PC, *et al.* (2000): The Autism Diagnostic Observation Schedule—Generic: A standard measure of social and communication deficits associated with the spectrum of autism. *J Autism Dev Disord* 30: 205–223.
 35. Gotham K, Pickles A, Lord C (2009): Standardizing ADOS scores for a measure of severity in autism spectrum disorders. *J Autism Dev Disord* 39:693–705.
 36. Liu Z, Wang Y, Gerig G, Gouttard S, Tao R, Fletcher T, Styner M (2010): Quality control of diffusion weighted images. *Proc SPIE Int Soc Opt Eng* 11:7628.
 37. Caramanos Z, Fonov VS, Francis SJ, Narayanan S, Pike GB, Collins DL, *et al.* (2010): Gradient distortions in MRI: Characterizing and correcting for their effects on SIENA-generated measures of brain volume change. *Neuroimage* 49:1601–1611.
 38. Behrens T, Berg HJ, Jbabdi S, Rushworth M, Woolrich M (2007): Probabilistic diffusion tractography with multiple fibre orientations: What can we gain? *Neuroimage* 34:144–155.
 39. Klein A, Tourville J (2012): 101 labeled brain images and a consistent human cortical labeling protocol. *Front Neurosci* 6:171.
 40. Fonov V, Evans AC, Botteron K, Almli CR, McKinstry RC, Collins DL, *et al.* (2011): Unbiased average age-appropriate atlases for pediatric studies. *Neuroimage* 54:313–327.
 41. Behrens T, Johansen-Berg H, Woolrich M, Smith S, Wheeler-Kingshott C, Boulby P, *et al.* (2003): Non-invasive mapping of connections between human thalamus and cortex using diffusion imaging. *Nat Neurosci* 6:750–757.
 42. Rubinov M, Sporns O (2010): Complex network measures of brain connectivity: Uses and interpretations. *Neuroimage* 52:1059–1069.
 43. Akaike H (1976): An information criterion (AIC). *Math Sci* 14:5–9.
 44. Posada D, Buckley TR (2004): Model selection and model averaging in phylogenetics: Advantages of Akaike information criterion and Bayesian approaches over likelihood ratio tests. *Syst Biol* 53: 793–808.
 45. Couteur A, Bailey A, Goode S, Pickles A, Gottesman I, Robertson S, *et al.* (1996): A broader phenotype of autism: The clinical spectrum in twins. *J Child Psychol Psychiatry* 37:785–801.
 46. Piven J, Palmer P, Jacobi D, Childress D, Arndt S (1997): Broader autism phenotype: Evidence from a family history study of multiple-incidence autism families. *Am J Psychiatry* 154:185–190.
 47. Bailey A, Palferman S, Heavey L, Le Couteur A (1998): Autism: The phenotype in relatives. *J Autism Dev Disord* 28:369–392.
 48. Piven J, Palmer P (1999): Psychiatric disorder and the broad autism phenotype: Evidence from a family study of multiple-incidence autism families. *Am J Psychiatry* 156:557–563.
 49. Benjamini Y, Hochberg Y (1995): Controlling the false discovery rate: A practical and powerful approach to multiple testing. *J R Stat Soc Series B Stat Methodol* 57:289–300.
 50. Rutter M (1978): Diagnosis and definition of childhood autism. *J Autism Child Schizophr* 8:139–161.
 51. Wetherby AM, Woods J, Allen L, Cleary J, Dickinson H, Lord C (2004): Early indicators of autism spectrum disorders in the second year of life. *J Autism Dev Disord* 34:473–493.
 52. Tager-Flusberg H (1981): On the nature of linguistic functioning in early infantile autism. *J Autism Dev Disord* 11:45–56.
 53. Schultz RT (2005): Developmental deficits in social perception in autism: The role of the amygdala and fusiform face area. *Int J Dev Neurosci* 23:125–141.
 54. Schultz RT, Gauthier I, Klin A, Fulbright RK, Anderson AW, Volkmar F, *et al.* (2000): Abnormal ventral temporal cortical activity during face discrimination among individuals with autism and Asperger syndrome. *Arch Gen Psychiatry* 57:331.
 55. Redcay E (2008): The superior temporal sulcus performs a common function for social and speech perception: Implications for the emergence of autism. *Neurosci Biobehav Rev* 32:123–142.
 56. Schultz RT, Grelotti DJ, Klin A, Kleinman J, Van der Gaag C, Marois R, Skudlarski P (2003): The role of the fusiform face area in social cognition: Implications for the pathobiology of autism. *Philos Trans R Soc Lond B Biol Sci* 358:415–427.
 57. Johnson MH, Griffin R, Csibra G, Halit H, Farroni T, De Haan M, *et al.* (2005): The emergence of the social brain network: Evidence from typical and atypical development. *Dev Psychopathol* 17:599–619.
 58. Leekam SR, Nieto C, Libby SJ, Wing L, Gould J (2007): Describing the sensory abnormalities of children and adults with autism. *J Autism Dev Disord* 37:894–910.
 59. Tomchek SD, Dunn W (2007): Sensory processing in children with and without autism: A comparative study using the short sensory profile. *Am J Occup Ther* 61:190–200.
 60. Crane L, Goddard L, Pring L (2009): Sensory processing in adults with autism spectrum disorders. *Autism* 13:215–228.
 61. Belmonte MK, Cook E, Anderson GM, Rubenstein JL, Greenough WT, Beckel-Mitchener A, *et al.* (2004): Autism as a disorder of neural information processing: Directions for research and targets for therapy. *Mol Psychiatry* 9:646–663.
 62. Courchesne E, Pierce K (2005): Why the frontal cortex in autism might be talking only to itself: Local over-connectivity but long-distance disconnection. *Curr Opin Neurobiol* 15:225–230.
 63. Whitehouse AJ, Bishop DV (2008): Do children with autism 'switch off' to speech sounds? An investigation using event-related potentials. *Dev Sci* 11:516–524.
 64. Sultan F, Augath M, Hamodeh S, Murayama Y, Oeltermann A, Rauch A, *et al.* (2012): Unravelling cerebellar pathways with high temporal precision targeting motor and extensive sensory and parietal networks. *Nat Commun* 3:924.
 65. Velasco M, Velasco F (1986): Subcortical correlates of the somatic, auditory and visual vertex activities. II. Referential EEG responses. *Electroencephalogr Clin Neurophysiol* 63:62–67.
 66. Velasco M, Velasco F, Olvera A (1985): Subcortical correlates of the somatic, auditory and visual vertex activities in man. I. Bipolar EEG responses and electrical stimulation. *Electroencephalogr Clin Neurophysiol* 61:519–529.

67. Landa R, Garrett-Mayer E (2006): Development in infants with autism spectrum disorders: A prospective study. *J Child Psychol Psychiatry* 47:629–638.
68. Yirmiya N, Ozonoff S (2007): The very early autism phenotype. *J Autism Dev Disord* 37:1–11.
69. Zwaigenbaum L (2010): Advances in the early detection of autism. *Curr Opin Neurol* 23:97–102.
70. Elsabbagh M, Johnson MH (2016): Autism and the social brain: The first-year puzzle. *Biol Psychiatry* 80:94–99.
71. Lewis JD, Theilmann RJ, Townsend J, Evans AC (2013): Network efficiency in autism spectrum disorder and its relation to brain overgrowth. *Front Hum Neurosci* 7:845.
72. Belmonte MK, Gomot M, Baron-Cohen S (2010): Visual attention in autism families: 'Unaffected' sibs share atypical frontal activation. *J Child Psychol Psychiatry* 51:259–276.
73. Massand E, Karmiloff-Smith A, Mitchell KJ (2015): Cascading genetic and environmental effects on development: Implications for intervention. In: Mitchell KJ, editor. *The Genetics of Neurodevelopmental Disorders*. Hoboken: Wiley-Blackwell, 275–288.
74. De Rubeis S, He X, Goldberg AP, Poultney CS, Samocha K, Cicek AE, *et al.* (2014): Synaptic, transcriptional and chromatin genes disrupted in autism. *Nature* 515:209–215.
75. Tang G, Gudsnek K, Kuo S-H, Cotrina ML, Rosoklija G, Sosunov A, *et al.* (2014): Loss of mTOR-dependent macroautophagy causes autistic-like synaptic pruning deficits. *Neuron* 83:1131–1143.
76. Auerbach BD, Osterweil EK, Bear MF (2011): Mutations causing syndromic autism define an axis of synaptic pathophysiology. *Nature* 480:63–68.
77. Nelson KB, Grether JK, Croen LA, Dambrosia JM, Dickens BF, Jelliffe LL, *et al.* (2001): Neuropeptides and neurotrophins in neonatal blood of children with autism or mental retardation. *Ann Neurol* 49:597–606.
78. Valla JM, Belmonte MK (2013): Detail-oriented cognitive style and social communicative deficits, within and beyond the autism spectrum: Independent traits that grow into developmental interdependence. *Dev Rev* 33:371–398.
79. Gogtay N, Giedd JN, Lusk L, Hayashi KM, Greenstein D, Vaituzis AC, *et al.* (2004): Dynamic mapping of human cortical development during childhood through early adulthood. *Proc Natl Acad Sci U S A* 101:8174–8179.
80. Bourne JA, Rosa MG (2006): Hierarchical development of the primate visual cortex, as revealed by neurofilament immunoreactivity: Early maturation of the middle temporal area (MT). *Cereb Cortex* 16:405–414.
81. Harris SL, Handleman JS (2000): Age and IQ at intake as predictors of placement for young children with autism: A four-to six-year follow-up. *J Autism Dev Disord* 30:137–142.
82. Dawson G, Rogers S, Munson J, Smith M, Winter J, Greenson J, *et al.* (2010): Randomized, controlled trial of an intervention for toddlers with autism: The Early Start Denver Model. *Pediatrics* 125:e17–e23.
83. Fenske EC, Zalsenski S, Krantz PJ, McClannahan LE (1985): Age at intervention and treatment outcome for autistic children in a comprehensive intervention program. *Anal Interv Dev Disabil* 5:49–58.
84. Makrygianni MK, Reed P (2010): A meta-analytic review of the effectiveness of behavioural early intervention programs for children with autistic spectrum disorders. *Res Autism Spectr Disord* 4:577–593.
85. Zhou X, Lu JY, Darling RD, Simpson KL, Zhu X, Wang F, *et al.* (2015): Behavioral training reverses global cortical network dysfunction induced by perinatal antidepressant exposure. *Proc Natl Acad Sci U S A* 112:2233–2238.